

## ATOMIC EFFECTS IN EXAFS STRUCTURAL ANALYSIS OF MIXED Ce OXIDE THIN FILMS

Jana Padežnik Gomilšek,<sup>a</sup> Alojz Kodre,<sup>b,c</sup> Nataša Bukovec,<sup>d</sup>  
and Irena Kozjek Škofic<sup>d</sup>

<sup>a</sup> Faculty of Mechanical Engineering, Smetanova 17, SI-2000 Maribor, Slovenia

<sup>b</sup> Faculty of Mathematics and Physics, Jadranska 19, SI-1000 Ljubljana, Slovenia

<sup>c</sup> Institute Jožef Stefan, Jamova 39, SI-1000 Ljubljana, Slovenia

<sup>d</sup> Faculty of Chemistry and Chemical Technology, Aškerčeva 5, SI-1000 Ljubljana, Slovenia

Received 17-10-2003

### Abstract

Standard structural analysis of cerium compounds by EXAFS (Extended X-Ray Absorption Fine Structure) is unreliable due to particularly strong multielectron photoexcitations (MPE). The collection of the MPE in the pure atomic signal of Ce, to be removed before the procedure, has not been measured or calculated *ab initio*; our suggestion is to transfer it from another Ce sample. An estimate of MPE contribution is extracted from the absorption spectrum of a Ce compound with known structure by removing the structural signal, calculated *ab initio*. In a combined fitting procedure of spectra of different compounds, the MPE estimate is refined. Using specific Ce<sup>3+</sup> and Ce<sup>4+</sup> estimates, absorption spectra of Ce oxide films are prepared free of the major part of MPE signal, especially of its long-wave components, so that a regular EXAFS analysis of the samples is possible.

**Key words:** EXAFS, Cerium, Electrochemistry

### Introduction

Thin films of ceria (CeO<sub>2</sub>) and mixed Ce/V oxides have been extensively studied as candidates for optically passive counter electrodes in electrochromic devices. Pure ceria is highly promising for its high transparency in the visible region in both reduced and oxidized state. It also shows a good reversibility of lithium intercalation, but a poor charge capacity.<sup>1-5</sup> Vanadium pentoxide, V<sub>2</sub>O<sub>5</sub>, on the other side, exhibits an appropriate charge capacity.<sup>6</sup> Its major drawback is the unfavorable brownish-grey coloration in the state with lithium intercalation. The mixture of both oxides is sought in which the advantages of both constituents would be retained and the drawbacks suppressed.<sup>7,8</sup>

The optical and electrochemical properties of ceria and Ce/V oxide films formed by the sol-gel route depend on the preparation mode, most notably on the annealing atmosphere and temperature and on the Ce/V molar ratio of the mixed oxides.<sup>9,10</sup> For

instance, annealing in argon at appropriate temperatures significantly improves ion storage capacity and cycling stability of the films. These electrochemical properties are expected to correlate with the local structure around the constituent metal ions. To elucidate this question, EXAFS analysis of the films was performed. Due to exceptionally strong intra-atomic effects in Ce, the analysis is not a routine operation. In this work we concentrate on the application of EXAFS method to Ce compounds while the resulting structural parameters of the films are discussed elsewhere.<sup>11</sup>

### Experiment

CeO<sub>2</sub>, Ce(NH<sub>4</sub>)<sub>2</sub>(NO<sub>3</sub>)<sub>6</sub> and CeCl<sub>3</sub>·7H<sub>2</sub>O were purchased from Fluka and CeCl<sub>3</sub>·7H<sub>2</sub>O was recrystallized from water before use. CeVO<sub>4</sub> was prepared by a procedure, compiled and combined from several sources.<sup>12-14</sup> Thin films of CeO<sub>2</sub> and Ce/V mixed oxide were prepared by sol-gel deposition on Al-foil and annealed in air or argon atmosphere.<sup>9,10</sup> Standard cerium L<sub>3</sub> EXAFS spectra were measured at the E4 experimental station of Hasylab (DESY) in Hamburg, Germany. A stack of 10 foils with double films (each ~80 nm thick) yielded the Ce L<sub>3</sub>-edge jump  $\Delta\mu/\mu_{L3}$  of ~0.2. Samples of CeO<sub>2</sub>, CeVO<sub>4</sub>, CeCl<sub>3</sub>·7H<sub>2</sub>O and Ce(NH<sub>4</sub>)<sub>2</sub>(NO<sub>3</sub>)<sub>6</sub> powders on adhesive tape with optimum edge jump of ~1 were measured for comparison. Energy calibration was established by a simultaneous measurement of metal Cr foil (K edge energy 5989 eV). Spectra were analyzed by FEFF6 code.<sup>15,16</sup>

### MPE in Ce EXAFS spectra

X-ray absorption cross-section above an inner-shell absorption edge of an element (at ~5730 eV for Ce L<sub>3</sub> edge in CeO<sub>2</sub> absorption spectrum, Figure 1) shows small deviations from the well-known smooth decrease with photon energy. The deviations are of twofold nature: *The structural signal* (EXAFS = extended X-ray absorption fine structure) comprises regular oscillations of absorption cross-section arising in the interference of the photoelectron wave with the waves scattered on the atoms in the neighborhood of the target atom. *The atomic signal* comprises irregular features, the fingerprints of coexcitations of valence and subvalence electrons in the process of core photoeffect (MPE = multielectron photoexcitations). Separately determined atomic signal of an element is known as the *atomic absorption background* (AAB).

Usually, the structural signal is much stronger than the MPE signal so that EXAFS analysis of the local structure of the sample around the target atom can be performed directly from the absorption spectrum. The first step of the procedure is to remove a smooth standard spline background from absorption data so that only the EXAFS oscillations remain, ready for harmonic analysis. In cerium, however, this procedure is not straightforward due to exceptionally strong double-electron transition  $2p_{3/2}4d$ :<sup>17,18</sup> an estimate of its contribution to the absorption spectrum obtained by Kodre *et al*<sup>18</sup> is shown in the inset in Figure 1. The MPE feature approximately 130 eV above the  $L_3$  edge is comparable in amplitude to the strong  $CeO_2$  structural signal and cannot be absorbed into the spline background of the spectrum. As a consequence, structural parameters obtained in the analysis are affected to that extent that quantitative analysis of Ce compounds is preferably avoided.<sup>19</sup>

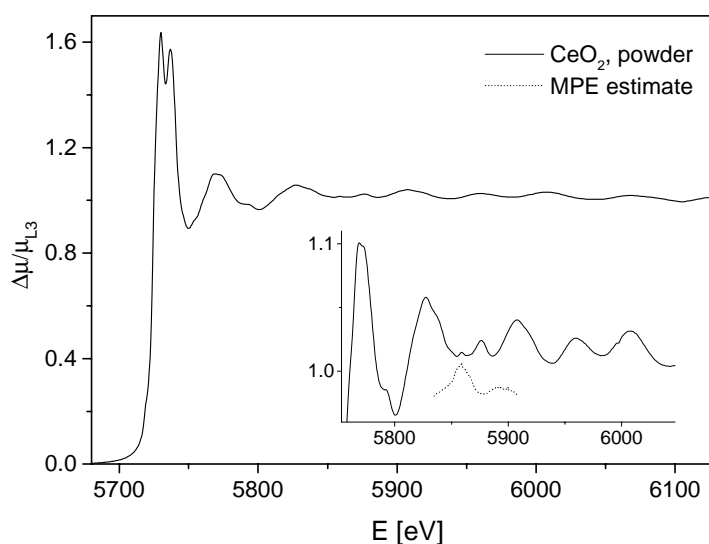


**Figure 1.** Normalized  $L_3$  edge absorption spectrum of  $CeO_2$  powder. In the inset a part of the above edge region is magnified and the absorption signal is compared to the estimate of  $2p_{3/2}4d$  MPE,<sup>18</sup> arbitrary shifted along y-axis.

A reliable EXAFS analysis of Ce spectra demands extraction of the MPE contribution before or simultaneously with the spline extraction. The MPE contribution is a consequence of collective motion of electrons in the atomic system and has not been measured or calculated for Ce with the desired precision. In a study of simple water solutions of Ce salts<sup>17</sup> it was found that the MPE features depend on the oxidation state of the Ce ion. The total strength of  $Ce^{3+}$  and  $Ce^{4+}$  MPE contributions is similar but the

shape is different: one peak is observed in  $\text{Ce}^{3+}$  compounds and two peaks in  $\text{Ce}^{4+}$  compounds. The dependence on the charge state can be explained by the fact that the MPE contribution in the X-ray absorption spectra arises from interactions within the target (cerium) atom and not from its chemical surroundings. The transferability of MPE features between spectra of different compounds of an ion with a particular oxidation state was further confirmed experimentally on some other compounds.<sup>20</sup>

A few approaches have been suggested to solve the MPE problem in Ce structural analysis:

- Lee *et al.*<sup>21</sup> suggest to switch from standard Ce  $L_3$ -edge EXAFS analysis to Ce K-edge. The total accessible  $L_3$  signal range is limited by the proximity of  $L_2$  edge to ~400 eV while at the isolated K edge more than 1000 eV can be analyzed and the effect of the MPE disturbance in a short (<100 eV) interval is diluted. The solution is not widely applicable because the energy threshold for K shell ionization (40443 eV) is out of range of most EXAFS beamlines.

- Kodre *et al.*<sup>18</sup> give an estimate of  $\text{Ce}^{3+}$  MPE signal to be used in analysis of other  $\text{Ce}^{3+}$  spectra. The estimate has been extracted from a simple EXAFS spectrum of Ce(III)-Ti citrate xerogel by modeling its EXAFS signal.

- Fonda *et al.*<sup>22</sup> performed a simultaneous analysis of  $\text{CeO}_2$  signal at all three L edges and at the K edge. The common  $\text{Ce}^{4+}$  MPE signal was approximated by a single Lorentzian with adjustable parameters: the height of 3.4% of the edge jump and the width of 10.7 eV were determined in the best-fit procedure. The complexity of the EXAFS signal of the well-ordered  $\text{CeO}_2$  system prevented to extract a better approximation of the two-peak feature seen in simpler EXAFS spectra of the element.<sup>17</sup>

In this work, we use a combined fitting procedure of spectra of different compounds to determine the  $\text{Ce}^{4+}$  MPE estimate. Both  $\text{Ce}^{3+}$  and  $\text{Ce}^{4+}$  MPE estimates are needed in EXAFS analysis of our thin films spectra since they contain both ionic species, as evidenced by the inspection of the edge profiles. The near edge region of the spectra of reference Ce compounds with different oxidation states are shown in Figure 2a. Evidently, all  $\text{Ce}^{3+}$  compounds show one prominent peak while  $\text{Ce}^{4+}$  spectra exhibit a two-peak feature with a point of maximum positive slope (= inflection point) approximately 4 eV higher than in  $\text{Ce}^{3+}$ . When the edges of Ce and Ce/V oxide films are similarly plotted (Figure 2b), some are recognized as 3+ and some as 4+. There is even a

sample with specific stoichiometry and annealing atmosphere to which an intermediate valence of 3.7 is attributed.

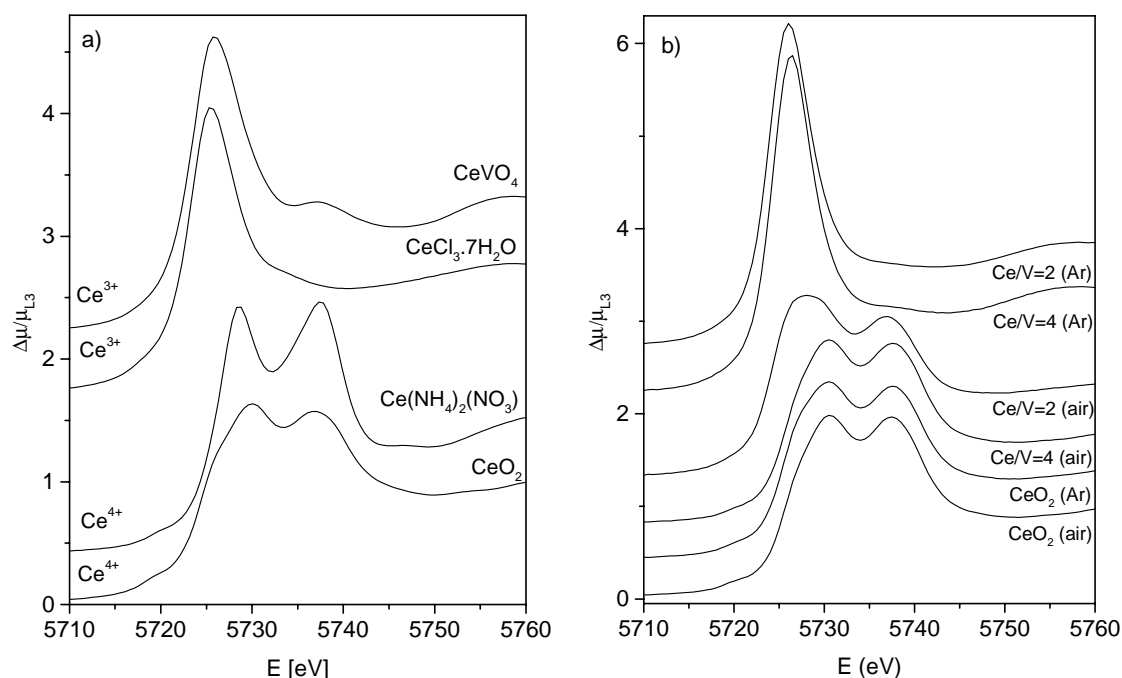


**Figure 2.** XANES (= X-ray absorption near edge structure) spectra of a) reference compounds, b) CeO<sub>2</sub> and mixed Ce/V oxide thin films.

### Determination of Ce<sup>4+</sup> MPE estimate

Spectra of CeO<sub>2</sub> and Ce(NH<sub>4</sub>)<sub>2</sub>(NO<sub>3</sub>)<sub>6</sub> reference powders were used to determine Ce<sup>4+</sup> MPE contribution. In the region where 2p<sub>3/2</sub>4d MPE are theoretically predicted, two small and narrow peaks are observed (vertical lines in Figure 3), superposed upon the long-wave oscillation of the structural signal. At first sight, it is not obvious that the MPE feature in both spectra is the same. However, it should be noted that the dominant (EXAFS) contribution is a complex interference of modulated harmonic signals arising from subsequent shells of neighbors and a simple observation can be misleading, especially for features in the vicinity of EXAFS peaks or valleys.

Recognizing the two-peak feature in both spectra as a single MPE, our task is to reverse the superposition and separate the EXAFS and MPE. A unique solution of the task is only possible with the requirement that the structural signals for the two known Ce neighborhoods are obtained after removal of the same MPE. In the exchange-fitting

procedure<sup>23</sup> the successive approximations of the MPE from one spectrum are used to solve the structural problem of the other sample and regain the next MPE approximation.

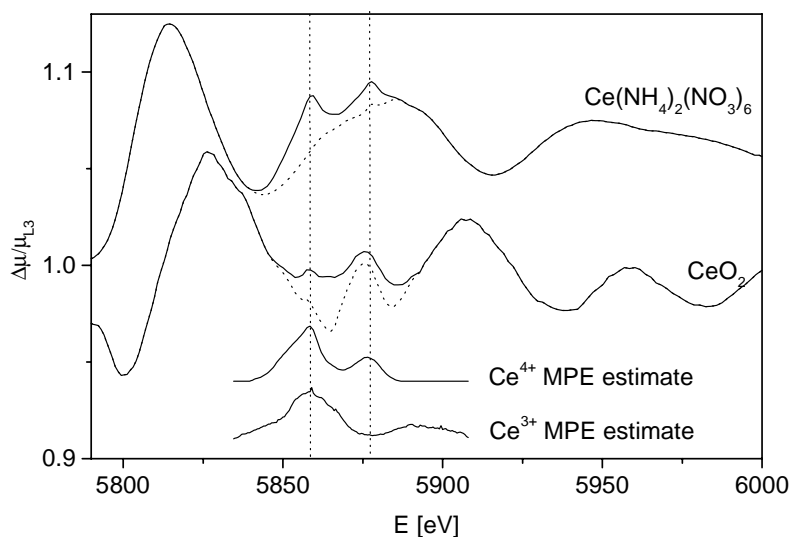


**Figure 3.** Spectra of reference  $\text{Ce}^{4+}$  compounds in the vicinity of the  $2p_{3/2}4d$  MPE feature with initial ( $\text{Ce}^{3+}$ ) and refined ( $\text{Ce}^{4+}$ ) MPE estimate. Dotted lines represent MPE corrected data (= original data –  $\text{Ce}^{4+}$  MPE estimate).

In the present case, the  $\text{Ce}^{3+}$  MPE estimate<sup>18</sup> is taken for the starting approximation: although the shape of the MPE contribution in  $\text{Ce}^{4+}$  is different, the total strength is approximately the same for both oxidation states. The energy position of this, basically one-peak feature, was slightly adjusted to coincide with one of the MPE peaks in the EXAFS spectra, namely the first peak as suggested by the simpler case of  $\text{Ce}(\text{NH}_4)_2(\text{NO}_3)_6$  spectrum. After the initial estimate was extracted from the absorption spectrum, a standard EXAFS analysis was performed based on the crystallographic data.<sup>24</sup> The best-fit model was then subtracted from the original data; the difference spectra in the 5830–5900 eV region is the first  $\text{Ce}^{4+}$  MPE estimate. The first peak, in particular, sitting on the slope of the EXAFS signal, is reliably reproduced after the subtraction, while the amplitude of the second peak remains poorly determined.

This estimate is used in the analysis of the  $\text{CeO}_2$  spectrum: here the first peak of the MPE feature is more ambiguous, filling up the EXAFS signal valley. The procedure is repeated and the final  $\text{Ce}^{4+}$  MPE estimate is determined. It consists of two peaks and can be roughly described as a sum of two lorentzian resonances 20 eV apart (at 5857 eV and 5877 eV, Figure 4) with amplitudes 2.7% and 1.1% of the main edge and the widths

12 eV and 7 eV, respectively. For comparison, the dominant peak in the  $\text{Ce}^{3+}$  MPE estimate (at 5852 eV) is  $\sim 2.5\%$  high and  $\sim 17$  eV wide. The shapes of both  $2p_{3/2}4d$  MPE features resemble the profiles of the respective main edges in Figure 2a.

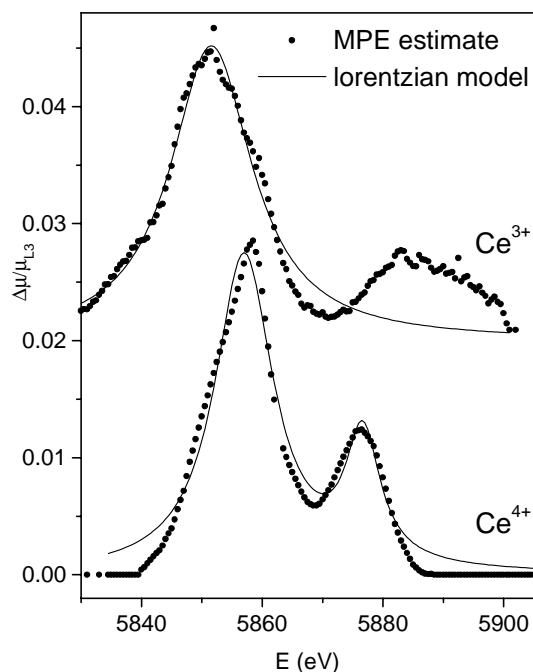


**Figure 4.**  $\text{Ce}^{3+}$  and  $\text{Ce}^{4+}$  MPE estimates and their approximation with Lorentzian resonances.

The obtained  $\text{Ce}^{4+}$  MPE estimate is ready to be subtracted from absorption spectra of other  $\text{Ce}^{4+}$  compounds prior to EXAFS analysis. Let us first see the effect on the reference spectra: the MPE corrected data are shown in Figure 3 by dotted lines. Obviously, the correction in the  $\text{Ce}(\text{NH}_4)_2(\text{NO}_3)_6$  spectrum is not perfect. Nevertheless, we believe that the long-wave part of the MPE contamination is mostly removed while small discrepancies in the short-wave region may persist. Since the structural parameters of near neighbors are determined mostly from the long-wave components of the EXAFS signal, we expect that the reliability of the structural analysis is strongly improved.

Owing to its large amplitude, the MPE contribution strongly affects the long-wave component as can be seen in Figure 5a for  $\text{CeO}_2$  thin film annealed in argon. Here, the EXAFS signal is especially low due to the high degree of disorder in the structure: the MPE contribution completely fills up the valley at  $\sim 5860$  eV, leading to a pronounced deformation of the background spline so that EXAFS amplitude is underestimated. The

effect in the  $r$ -space is shown in Figure 5b. Here the energy scale of Figure 5a is converted to the photoelectron wavenumber  $k$  scale ( $E - E_o = \frac{\hbar^2 k^2}{2m}$ ;  $E_o = 5731$  eV is the energy of  $L_3$  edge) and Fourier transform of the data is performed. This presentation of EXAFS data is the starting point for the best-fit adjustment of the structural parameters. The  $r$  coordinate is simply the distance from the central Ce atom, and the peaks in the FT plot represent roughly the probability that a neighbor is found in the ( $r$ ,  $r+dr$ ) interval. So the first peak in Figure 5b consists of long wave signal components arising from the first neighbors. In the presence of the MPE contribution, the low- $r$  flank of the peak is deformed and the amplitude is suppressed leading to large shifts in the model parameters.

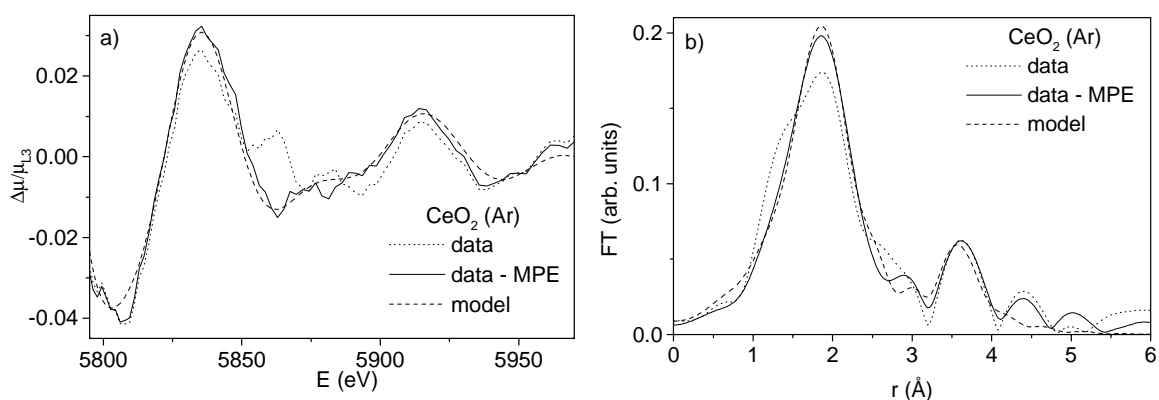


**Figure 5.** E- and  $r$ -space EXAFS data for  $\text{CeO}_2$  thin film annealed in argon. Original and MPE corrected data are presented together with the best-fit model.

## Conclusions

An estimate of the strong  $2p_{3/2}4d$  MPE in the  $\text{Ce}^{4+}$  was determined by modelling  $\text{CeO}_2$  and  $\text{Ce}(\text{NH}_4)_2(\text{NO}_3)_6$  data and using  $\text{Ce}^{3+}$  MPE estimate<sup>18</sup> as the starting approximation. So MPE estimates for both Ce ions are available and any Ce compound can be analysed after subtraction of the adequate MPE estimate from the normalized absorption data. Since MPE features in Ce are unusually strong the procedure is indispensable for reliable determination of structural parameters.

In most cases, the long wave components of EXAFS signal are of interest and subtracting simple Lorentzian resonances is sufficient. One Lorentzian is needed for  $\text{Ce}^{3+}$



compounds and two for Ce<sup>4+</sup> compounds, the parameters are given in this work. For Ce<sup>4+</sup>, the suggestion of the MPE estimate by Fonda *et al.*<sup>22</sup> is in fair agreement with the first Lorentzian in our estimate, but the authors fail to recognize the oxidation-state dependence of the MPE.

### Acknowledgements

This work was supported by the Ministry of Education, Science and Sport of the Republic of Slovenia (P1-0134, J1-3392-0795-01) and the IHP-Contract HPRI-CT-1999-00040 of the European Commission. Advice on beamline operation by Konstantin Klementiev of HASYLAB is gratefully acknowledged.

### References

1. N. Özer, *Solar Energy Mater. Solar Cells* **2001**, 68, 391–400.
2. B. El Idrissi, M. Addou, A. Outzourhit, M. Regragui, A. Bougrine, A. Kachouane, *Solar Energy Mater. Solar Cells* **2001**, 69, 1–8.
3. M. Veszelei, M. Strømme Mattsson, L. Kullman, A. Azens, C. G. Granqvist, *Solar Energy Mater. Solar Cells* **1999**, 56, 223–230.
4. D. Kéomany, J.-P. Petit, D. Deroo, *Solar Energy Mater. Solar Cells* **1995**, 36, 397–408.
5. U. Lavrenčič Štangar, B. Orel, I. Grabec, B. Ogorevc, K. Kalcher, *Solar Energy Mater. Solar Cells* **1993**, 31, 171–185.
6. C. G. Granqvist, *Handbook of Inorganic Electrochromic Materials*; Elsevier, Amsterdam, 1995, pp 295–338.
7. E. Masetti, F. Varsano, F. Decker, *Electrochim. Acta* **1999**, 44, 3117–3119.
8. U. Opara Kraševc, B. Orel, A. Šurca, N. Bukovec, R. Reisfeld, *Solid State Ionics* **1999**, 118, 195–214.
9. I. Kozjek Škofic, S. Šturm, M. Čeh, N. Bukovec, *Thin Solid Films* **2002**, 422, 170–175.
10. I. Kozjek Škofic, N. Bukovec, *Acta Chim. Slov.* **2002**, 49, 267–278.
11. J. Padežnik Gomilšek, I. Kozjek Škofic, N. Bukovec, A. Kodre, *Thin Solid Films* **2004**, 446, 117–123.
12. M. K. Carron, M. E. Mrose, K. J. Murata, *Am. Mineral.* **1958**, 43, 985–989.
13. C. Baudracco-Gritti, S. Quartieri, G. Vezzalini, F. Permingeat, F. Pillard, R. Rinaldi, *Bull. Minéral.* **1986**, 110, 657–672.
14. PDF-2, International Centre for Diffraction Data, Newtown Square, Pennsylvania USA, **2001**, File No 12–0757.
15. E. A. Stern, M. Newville, B. Ravel, Y. Yacoby, D. Haskel, *Physica B* **1995**, 208&209, 117–120.
16. J. Rehr, R. C. Albers, S. I. Zabinsky, *Phys. Rev. Lett.* **1992**, 69, 3397–3400.
17. J. A. Solera, J. Garcia, M. G. Proietti, *Phys. Rev. B* **1995**, 51, 2678–2686.
18. A. Kodre, I. Arčon, M. Hribar, M. Štuhec, F. Villain, W. Drube, L. Troeger, *Physica B* **1995**, 208&209, 379–380.
19. P. Nachimuthu, W.-C. Shih, R.-S. Liu, L.-Y. Jang, J.-M. Chen, *J. Solid State Chem.* **2000**, 149, 408–413.
20. A. Kodre, J. Padežnik Gomilšek, I. Arčon, R. Prešeren, *J. Synch. Radiat.* **1999**, 6, 306–307.
21. J.-F. Lee, M.-T. Tang, W. C. Shih, R. S. Liu, *Material Research Bulletin* **2002**, 37, 555–562.
22. E. Fonda, D. Andreatta, P. E. Colavita, G. Vlaic, *J. Synchrotron Rad.* **1999**, 6, 34–42.

23. J. Padežnik Gomilšek, A. Kodre, I. Arčon, A. M. Loireau-Lozac'h, S. Bénazeth, *Phys. Rev A* **1999**, 59, 3078–3081.
24. T. A. Beineke, J. Delgado, *Inorg. Chem.* **1968**, 7, 715–721.

### Povzetek

Standardna strukturna analiza EXAFS (podaljšana fina struktura rentgenskih robov) cerijevih spojin je nezanesljiva zaradi izredno močnih večelektronskih fotovzbuditev (MPE). Pred analizo bi namreč morali odstraniti prispevek MPE k absorpciji, vendar le-ta še ni izmerjen ali izračunan *ab initio*, zato predlagamo, da ga prenesemo iz meritev drugih cerijevih spojin. Uporabili smo približek MPE, izločen iz absorpcijskega spektra cerijeve spojine z znano strukturo, za katero je strukturni signal izračunan *ab initio*. Z izmenjalnim postopkom na različnih spojinah smo ta približek izboljšali. Približka MPE za  $Ce^{3+}$  in  $Ce^{4+}$ , ki vsebujeta večino signala MPE, predvsem njegov dolgovalovni del, sta omogočila analizo EXAFS vzorcev tankih filmov cerijevega oksida in mešanih oksidov Ce/V.